Open Access Journal
Journal of Power Technologies 92 (2) (2012) 115–126
journal homepage:papers.itc.pw.edu.pl

Novel sorbents for flue gas purification☆

Aleksandra Ściubidło*, Wojciech Nowak

Institute of Advanced Energy Technologies, Czestochowa University of Technology
73 Dabrowskiego Street, 42-201 Czestochowa, Poland

Abstract

This paper presents a method for cleaning exhaust gas of nitrogen oxides using the process of physical adsorption on novel sorbents obtained from fly ash. Use of this method, combined with CO_2 capture, allows emission standards to be met.

Keywords: sorbents, nitrogen oxides, mesoporous material MCM-41, physical adsorption, fly ash

1. Introduction

Due to the obligations arising from the European Union climate-energy package emphasis is placed on reducing greenhouse gas emissions, especially CO_2, which is considered a major cause of global warming. In accordance with the requirements of the European Commission, by the year 2020, CO_2 emissions should be reduced by 20%, the share of renewable energy sources (RES) should increase by 20%. Since the share of coal in total CO_2 emissions is approximately 38%, and since it is the main fuel for energy production in Poland, the most appropriate technologies seem to be carbon capture and storage (CCS). The European Commission stresses that carbon sequestration will be a necessary condition for using coal as a fuel.

Great emphasis is put on CO_2 removal from flue gas using two methods: the absorption method, and adsorption on amine solid sorbents modified with amines. The main problem associated with these methods is the pollution of amines with compounds such as oxides of sulfur and nitrogen. As a result of chemical reactions between oxides and amines, irreversible reactions take place which causes degradation of amines. In the case of SO_2, safe concentrations should not exceed 10 ppm, while for oxides of nitrogen they should be less than 40 mg/Nm^3 (20 ppm). In the case of nitrogen oxides, both methods of primary and secondary NO_x reduction fail to achieve safe concentrations of nitrogen oxides in the exhaust gas. The most effective way to reduce emissions of nitrogen oxides is the SCR method, which achieves emission limits of 100 mg/Nm^3. Unfortunately, this value is 5 times higher than that permissible for amines-based carbon capture.

The exhaust gas from a power plant boiler contains 95–97% NO, 3–5% NO_2, and about 0.5% N_2O. Because NO is an inert gas but easy to oxidize chemically, the author proposes to pick up the NO_2 in the process of adsorption on solid sorbents after first oxidizing NO to NO_2.

Sorbents such as mesoporous materials can be obtained, with benefits to the environment, from power

☆Paper presented at the 10th International Conference on Research & Development in Power Engineering 2011, Warsaw, Poland

*Corresponding author
Email addresses: asciubidlo@is.pcz.czest.pl (Aleksandra Ściubidło*), wnowak@is.pcz.czest.pl (Wojciech Nowak)

Table 1: Chemical composition of fly ash

Content of basic chemicals*, wt. %	
LOI	2.97
S	0.16
C	3.41
SiO_2	51.39
Al_2O_3	24.9
Fe_2O_3	3.72
CaO	4.35

*averaged values measured on a large sample

plant fly ash waste. Due to its chemical composition, fly ash is a valuable source of silicon and aluminum in the synthesis of mesoporous materials [1–8]. A number of applications of both microporous and mesoporous molecular sieve can be found in the literature. They are used among others in the purification of gases from pollutants such as carbon dioxide, sulfur dioxide, hydrogen sulfide, nitrogen oxides and mercury [2, 9–22]. In the case of materials synthesized from fly ash, information can also be found about their use in the purification of gases, mainly carbon dioxide, through adsorption.

This paper presents a method for cleaning exhaust gas of nitrogen oxides using the process of physical adsorption on novel sorbents obtained from fly ash. Use of this method, combined with CO_2 capture, allows emission standards to be met.

2. Experiment

2.1. Characteristics of the source material for the synthesis of the mesoporous material MCM-41

2.1.1. Chemical Composition

As a starting material fly ash derived from the combustion of coal in a pulverized boiler was used. The chemical composition of the fly ash was determined with use of an X-ray fluorescence spectrometer, and the results are presented in Table 1.

The ash had a SiO_2 content of 51.39 wt. %, 24.9 wt. % of Al_2O_3 and a CaO content of 4.35 wt. %. These data indicate that the ash in accordance can be classified as a silica ash (Polish standard BN-79/6722-09).

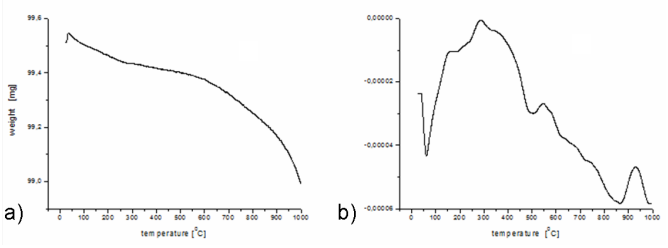

Figure 1: Thermogravimetric analysis TGA (a) and DTG (b) of fly ash

2.1.2. Thermogravimetric Analysis

The effect of temperature on the sample ash was investigated by the thermogravimetry method (TG) and differential thermal analysis (SDTA) using a Mettler Toledo TGA / SDTA 851e thermal analyzer. A sample of fly ash was heated in a platinum crucible at atmospheric pressure in an inert atmosphere (N_2) with a gas flow rate of 50 cm^3/min, in a temperature range of 293–1273 K with a heating speed 293 K/min. The weight of samples was 10 mg. The results of the studies, in the form of thermograms, are shown in Figure 1 as graphs illustrating the relationship between the weight change of a sample versus temperature (TG signal) and its first derivative (DTG).

The figure shows the three weight losses for the ash samples, with local minima at temperatures of 50°C, 500°C and 870°C respectively. The first loss is 0.02 mg, which is caused by water evaporation. The second loss, of 0.15 mg, is due to the dehydration of $Ca(OH)_2$. At 870°C there is a mass loss of 0.12 mg, resulting from the decomposition of $CaCO_3$. The total mass loss of the sample is 0.56 mg.

2.1.3. Analysis of the surface area

In order to examine the structure of fly ash, low-temperature nitrogen adsorption at 77 K was carried out on ASAP 2000 apparatus. After degassing the sample at 623 K the adsorption-desorption isotherms of nitrogen were measured. Based on these isotherms, the surface area, total pore volume, mean pore diameter, pore volume distribution as a function of their diameter and size distribution of surface area versus pore diameter were calculated.

Figure 2 shows adsorption/desorption isotherm curves as well as pore volume and size distribution of the surface as a function of their diameter. The

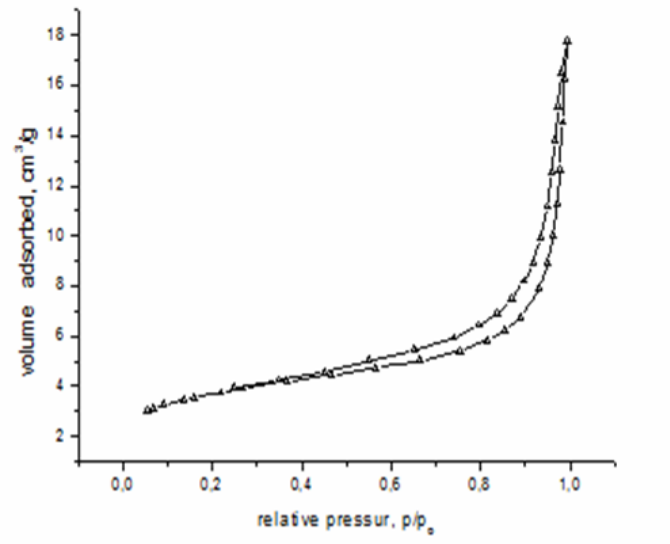

Figure 2: N2 adsorption/desorption isotherms for fly ash

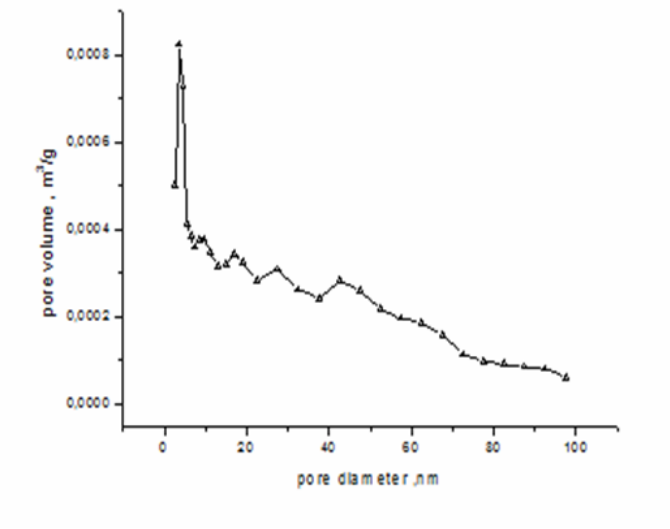

Figure 3: Pore size distribution of fly ash

presented adsorption/desorption isotherms of ash are consistent with the classification of IUPAC and these are the type II isotherms observed in macroporous adsorbents. From the presented curves can be seen that the adsorption is small at large values of $\frac{p}{p_0}$, and that the hysteresis loop, whose shape is related to the proper pore structure and which in this case can be classified as H3, starts at low relative pressures, indicating the small share of micropores in the structure.

Analyzing the distribution curves of pore volume by their diameter, as shown in Figure 3, it should be noted that the largest share of the total pore volume are pores with a diameter of 2.5–4.5 nm.

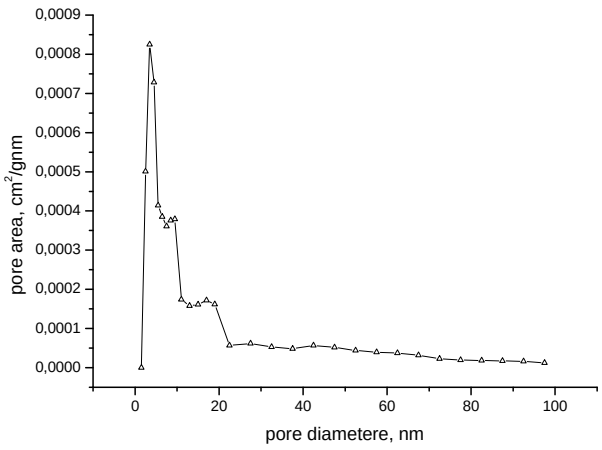

Figure 4: Surface area size distributions by pore size for the fly ash

Analyzing the distribution curves of specific surface as a function of pore diameter (Fig. 4), it should be noted that the largest share of the total surface area are pores with a diameter of 2.5–4.5 nm.

2.1.4. Images of the surface

In order to determine the shape and size of crystallite size in the range of 0.1–10 microns and its morphology and structure, fly ash samples were analyzed by scanning microscopy (SEM). The tests were performed using a Tesla BS-301 scanning electron microscope equipped with a Satellite digital imaging system.

The samples for SEM were prepared by spraying the surface of the tested materials with a thin layer of Au-Pd. Then digital images were taken with the SE detector microscope for various parts of the surface of these samples at different magnifications. Micrograms of the tested samples are shown in Fig. 5.

The presence of fly ash components such as SiO_2, calcium, and unburned carbon can be seen in these pictures.

2.2. Synthesis of mesoporous silica materials MCM-41

Extract from fly ash, a rich source of silicon and aluminum, is needed for the synthesis of MCM-41. To achieve this, the ashes were mixed with NaOH in a way allowing the mass ratio to remain at 1:1.2. Next the mixture was ground for 2 hours and then

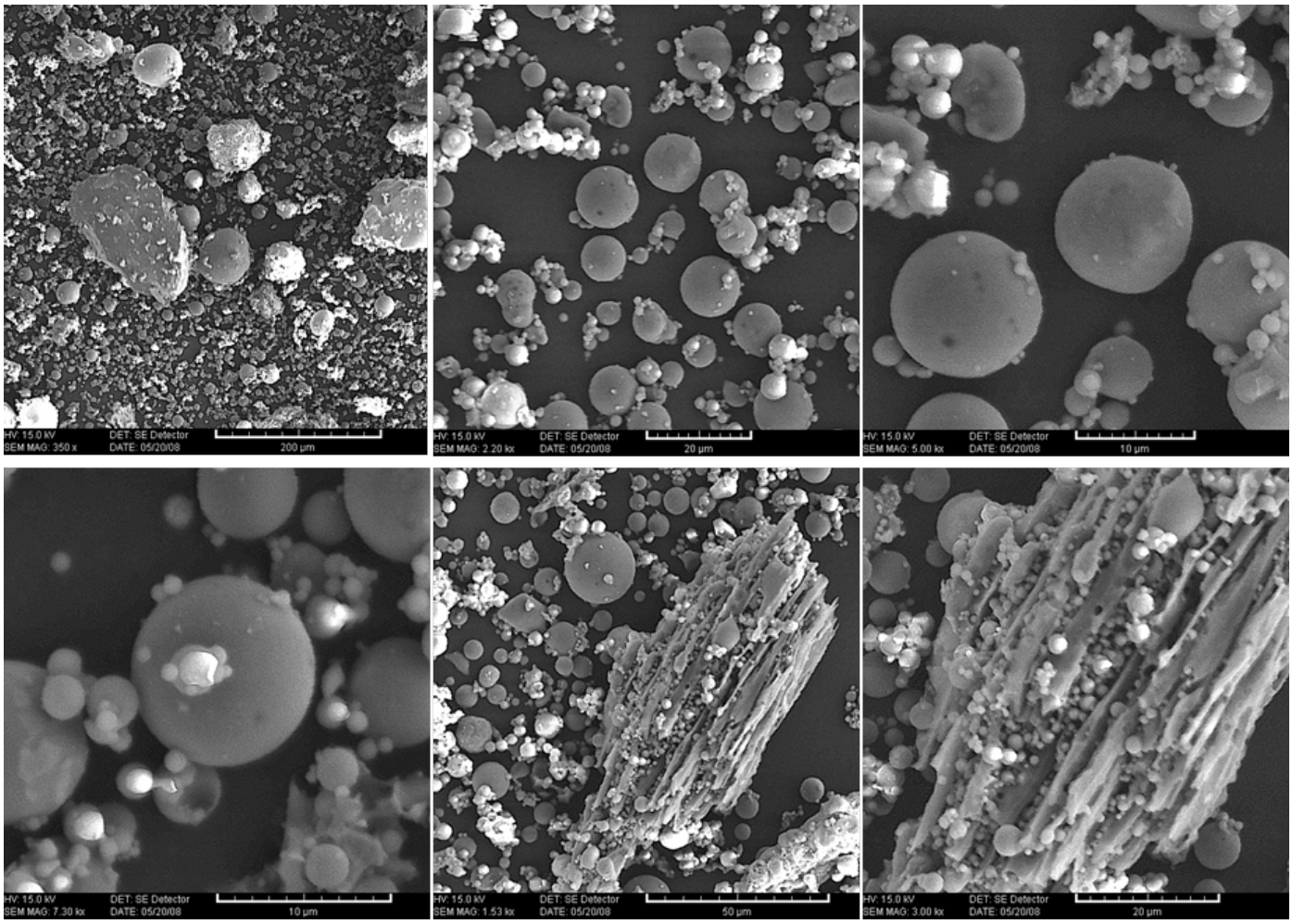

Figure 5: SEM images of fly ash

Table 2: Element concentrations in the filtrate

Elemental compositions	Concentration in the filtrate, mg/l
Fe	1.2
Na	$7.6 \cdot 10^4$
K	$1.9 \cdot 10^3$
Ca	12
Mg	0.2
Al	$8.4 \cdot 10^2$
Si	$1.96 \cdot 10^3$

the sample was subjected to heat treatment at 823 K for 1 hour with a heating speed of 1 K/min. After cooling to room temperature the material was ground again and mixed with water in a mass ratio of 1:4 the sample was shaken at room temperature for 12 hours. The sample was then filtered and the filtrate was subjected to ICP analysis. The results of the analysis are presented in Table 2.

The results shown in Table 2 show that the silicon content in solution was $1.96 \cdot 10^3$ mg/l and aluminum content was $8.4 \cdot 10^2$ mg/l. A surfactant-matrix solution was added to a previously prepared extracted solution of silicon. For this purpose, CTAB (cetyltrimethylammonium bromide—$C_{16}H_{33}(CH_3)_3NBr$) was dissolved in distilled water and NH_4OHaq was added. Next it was added to the supernatant (silicon extract) so that the molar ratio in the gel was SiO_2:CTAB:H_2O = 1:0.15:170. The pH of the solution was adjusted to 11 by adding CH_3COOH and it was adjusted several times while heating the mixture at 373 K for 4 days. The crystallized sample was then filtered and washed with distilled water to remove excess NaOH and dried at 373 K for 24 h. In order to remove the sample matrix it was calcined at 823 K for 2 hours with a heating speed of 1 K/min.

Figure 6 shows a picture of the mesoporous sieve MCM-41 that was finally obtained.

The adsorption properties of the obtained material were examined by nitrogen adsorption at 77 K, which enabled determination of the total surface area, total pore volume and pore volume distribution according to their diameter.

Table 3 shows the data obtained for the ash and the material obtained from it.

Figure 6: Picture of sieve MCM-41. The resulting material was subjected to tests to determine its physical and chemical properties

Table 3: Pore characteristics of fly ash and MCM-41

Sample	Pore volume, cm^3/g	Specific surface area SB.E.T., m^2/g	Pore diameter, nm
Ash	0.001	0.6	9.11
Material MCM-41	0.673	980	2.74

The SBET specific surface of fly ash was 0.6 m^2/g, total pore volume of 0.001 cm^3/g with an average pore radius of 9.11 nm. For the obtained material the specific surface SBET of fly ash was 980 m^2/g, total pore volume of 0.673 cm^3/g with an average pore radius of 2.74 nm.

The resulting material was also analyzed using a high-resolution D8 Advance Powder Diffractometer with a Ge monochromator (length radiated CuKα1 = 1.5406 $\mathring{A}$). Reflections were recorded with a LynxEye silicon strip detector. Measurements were performed using a cuvette made of polymethylmethacrylate. Diffraction patterns were recorded at room temperature for 10-70° 2Θ with steps of 0.0499, at 1 step/sec. During the measurements the sample was rotated at 30 rotations/minute. Measurements were performed at X-ray generator tube voltage of 35 kV and current of 50 mA.

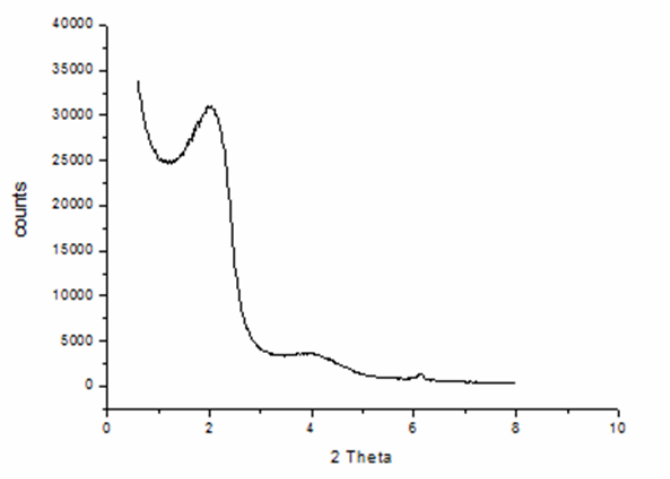

Figure 7: XRD pattern of the MCM-41(low angle)

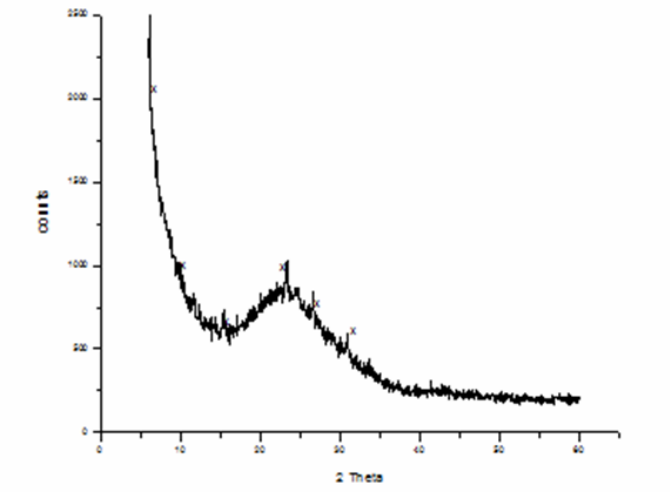

Figure 8: XRD pattern of the MCM-41(high angle)

Figures 7 and 8 show low and high angle diffraction patterns of the received material.

As can be seen from Figure 7, the low angle diffraction pattern contains the characteristic peak of mesoporous material MCM-41. In the sample material, the presence of pores with uniform mesopores and amorphous silica was observed.

The resulting material was also analyzed using scanning electron microscopy (SEM) to determine the morphology and porous structure. Preparations for SEM were prepared by spraying the surface of the tested materials with a thin layer of Au-Pd. Then the digital images of different parts of the surface of these preparations at different magnifications were taken with the microscope. Pictures of the tested samples are shown in Figure 9. SEM photos of mesoporous material from fly ash MCM-41 show that the material structure is mostly particle agglomeration. Photomicrographs show a regular arrangement of the channels.

In the pictures, the hexagonal structure of the resulting mesoporous material MCM-41 can be seen.

Both diffractometric and scanning analysis, as well as adsorption isotherms confirm that mesoporous material MCM-41 with a hexagonal structure was obtained.

2.3. Adsorption

In order to determine the suitability of obtained sorbents in the process of adsorption of NO_2, the sorption capacity characteristics of the NO_2 was determined. Figure 10 is a schematic diagram of the laboratory test rig on which the tests were performed. The position includes:

- Vertical tube furnace,
- Exhaust gas analyzer,
- Computer system of data acquisition,
- Rotameters,
- Mixer,
- Cylinders of gases.

Due to the limits for NO_x emission being set at the level of 200 mg/Nm^3, a mixture of air (21% O_2, 79% N_2) and nitrogen dioxide at concentrations of 50 ppm NO_2 (100 mg/Nm^3) and 100 ppm (200 mg/Nm^3) and gas consisting of 15% CO_2, 6% O_2 and 79% N_2 were used in the research. Tests were conducted at temperatures of: 25°C, 60°C and 80°C. The gas stream with a fixed volume flux regulated by the rotameter passed through the furnace tube, inside which sorbent was placed on the grate. After the gas passed through the sorbent, changes in concentrations were recorded by an IMR 6000P analyzer at intervals of 10 s. The range of the analyzer measuring NO_2 was 0–250 ppm, subrange 0.5% with an accuracy of + / - 1%. Sorption capacity was calculated on the basis of the weight of gas adsorbed on the sorbent (as well as by weighing the mass increase of the sample before and after the process) and expressed in mg of

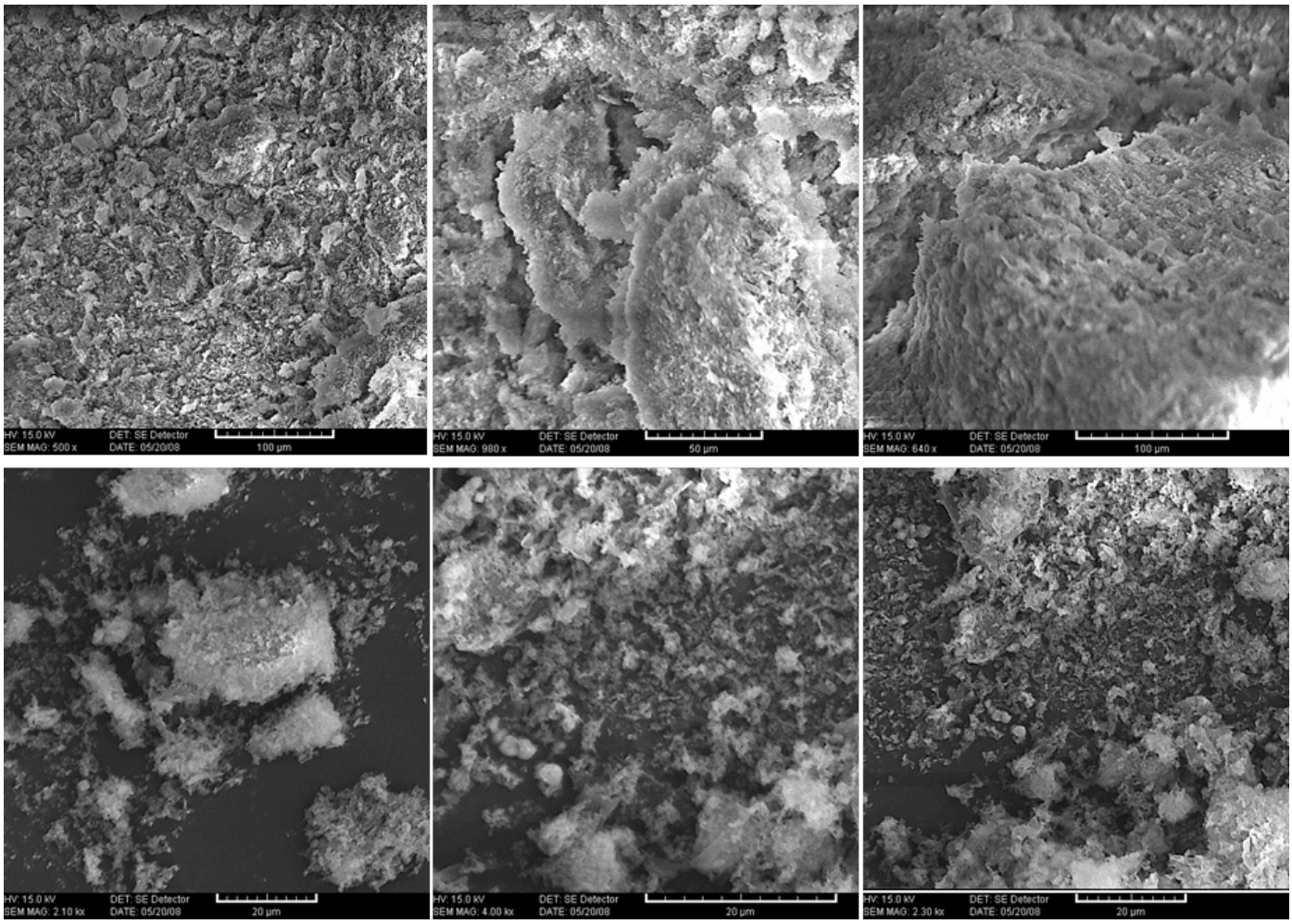

Figure 9: SEM images of MCM-41

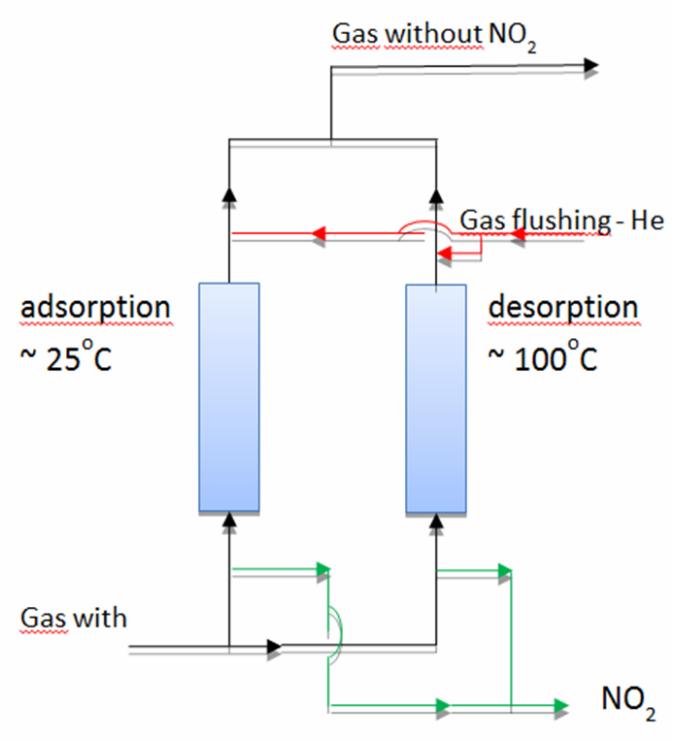

Figure 10: Diagram of the purification

gas per 1 g of sorbent. During the adsorption process the variable parameters were: temperature of the process, the NO_2 concentration and the presence of CO_2 in the gas mixture. The desorption process was conducted at 100°C in a helium flow. The tests were performed using MCM-41 sieve obtained from fly ash. Prior to use, the sieves were heated at 100°C temperature in a helium flow.

The adsorption process was conducted until the bed adsorption capacity was exhausted. From the results obtained, curves of NO_2 concentration as a function of time, called breakthrough curves, were created. They were used to calculate the mass of NO_2 adsorbed on the sorbent and the sorption capacity, expressed in mg NO_2/g of sorbent.

Figure 10 presents a diagram of the NO_2 removal process, involving the capture of nitrogen dioxide on solid sorbent obtained from fly ash.

The system consists of two columns filled with a suitable sorbent. Gas containing NO_2 enters the system and passes through the first column where, at a temperature of 25°C, the adsorption process takes place. When the adsorbent bed is exhausted, the desorption process is carried out at a temperature of

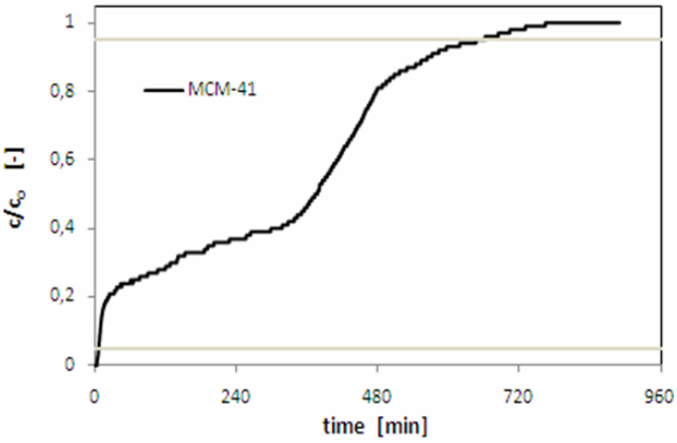

Figure 11: Breakthrough curves of NO_2/air for a sieve MCM-41 and MCM-41-PEG(50)

100°C in the presence of a helium gas flow. Desorbed gas is derived from the system. The continuity of the process is assured as the presented system consists of two columns, in which the adsorption-desorption processes take place alternately. The adsorption process occurs in the first column at the same time as the desorption process takes place in the second column.

2.3.1. Nitrogen dioxide adsorption on mesoporous sieve MCM-41

The sieve MCM-41 obtained from fly ash was used for testing purposes. NO_2 gas at a concentration of 100 ppm/air was passed through the bed (MCM-41).

The study was carried out at 25°C. The data obtained is used to plot changes in the concentration of NO_2 gas over time. The horizontal axis indicates the time of the adsorption process, and the ordinate axis the ratio of NO_2 gas concentration at the outlet of the column to the concentration of NO_2 supplied to the column. These curves are called breakthrough curves and the breakthrough time of the bed can be determined from them. The breakthrough time is required to calculate the mass of adsorbed gas on the sorbent and the sorption capacity of sorbent. Figure 11 shows the breakthrough curves of MCM-41 sieves at a concentration of 100 ppm NO_2.

The curve was used to calculate the sorption capacity of MCM-41 sieve at the level of 0.1 mg NO_2/g of sorbent.

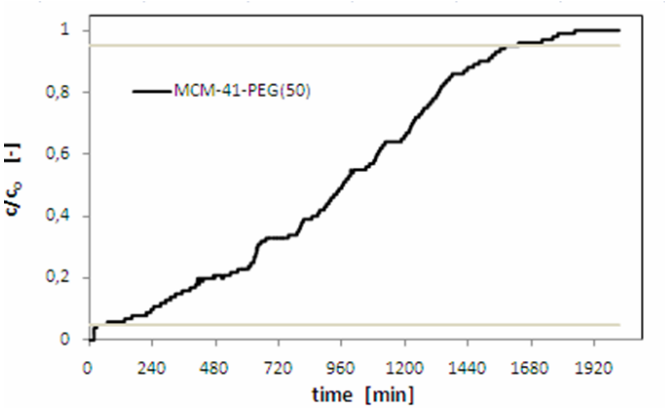

Figure 12: Breakthrough curves of NO_2/air for sieve MCM-41 and MCM-41-PEG(50)

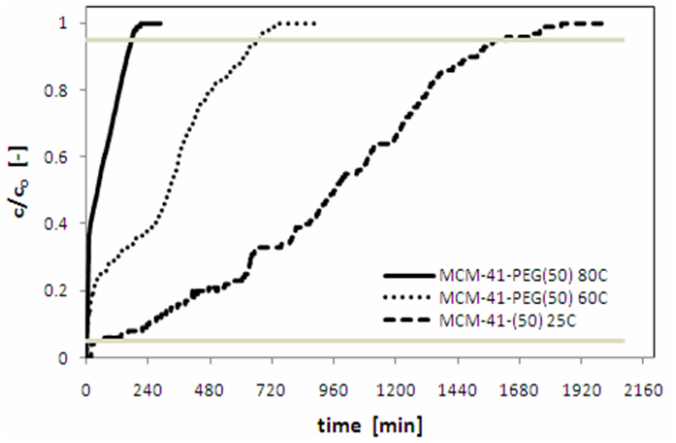

Figure 13: Breakthrough curves of NO2/air for a sieve MCM-41-PEG(50) at temperatures 25°C, 60°C and 80°C

Table 4: Sorption capacity

No.	sample	Sorption capacity of NO_2
1.	MCM-41	$mg/g_{sorbent}$
2.	MCM-41-PEG(50)	1.35

2.3.2. *Effect of impregnation with a solution of PEG on the sorption capacity of MCM-41 sieve*

To increase the sorption capacity and selectivity of the obtained material in terms of nitrogen dioxide, the sorbent was modified. This modification consisted of wet impregnation with polyethylene glycol solution.

The modification procedure was conducted as follows:

After dissolving 4 grams of PEG in 32 g of ethanol, 4 g calcined sieve MCM-41 was added. Subsequently, the sample was stirred for 8 hours and then the solution was evaporated. The resulting material was impregnated with 50% polyethylene glycol PEG and labeled MCM-41-PEG(50).

The prepared sorbent was subjected to the adsorption process at a temperature of 25°C while passing through a bed of sorbent NO_2 gas at a concentration of 100 ppm/air. Figure 12 shows the breakthrough curve of MCM-41-PEG(50) sieve. The curve was used to calculate the sorption capacity: for sieve MCM-41-PEG(50) it was 1.35 mg NO_2/g of sorbent.

Table 4 shows data collected from studies conducted for sieve MCM-41 and for its modification: MCM-41-PEG(50).

As can be seen, the sorption capacity of sieve whose surface has been modified was about 3 times greater than that of the unmodified sieve.

2.3.3. *The influence of temperature on the sorption capacity of MCM-41 sieve*

As the impregnated sorbent had a higher sorption capacity relative to NO_2 than the base sorbent (without impregnation), further tests were performed on the impregnated material MCM-41-PEG(50) to determine the effect of temperature and concentrations of NO_2 as well as the presence of synthetic gas.

The temperature influence on the sorption capacity was determined by measurements at the temperatures of: 25°C, 60°C, 80°C at a concentration of 100 ppm NO_2.

Figure 13 presents the breakthrough curves for sieve MCM-41-PEG(50) for temperatures: 25°C, 60°C and 80°C at a concentration of 100 ppm NO_2/air. Sorption capacity was calculated on the basis of breakthrough curves. At 25°C sorption capacity was 1.35 mg NO_2/g of sorbent, at the temperature of 60°C it was 0.11 mg NO_2/g of sorbent; the lowest sorption capacity was at the temperature of 80°C: 0.10 mg NO_2/g of sorbent.

Table 5 shows the sorption capacity of the sieve MCM-41-PEG(50) at different temperatures.

As can be seen from Table 5 and the results obtained, as the temperature rises the sorption capacity for sieve MCM-41PEG(50) decreases. The largest sorption capacity of the material was at 25°C, while

Table 5: Sorption capacity for sieve MCM-41-PEG(50)

No.	Sorbent	Temperature, °C	Sorption capacity of NO_2, $mg/g_{sorbent}$
1.	M	25	1.35
2.	CM-	60	0.11
3.	41-	80	0.1
	PEG(50)		

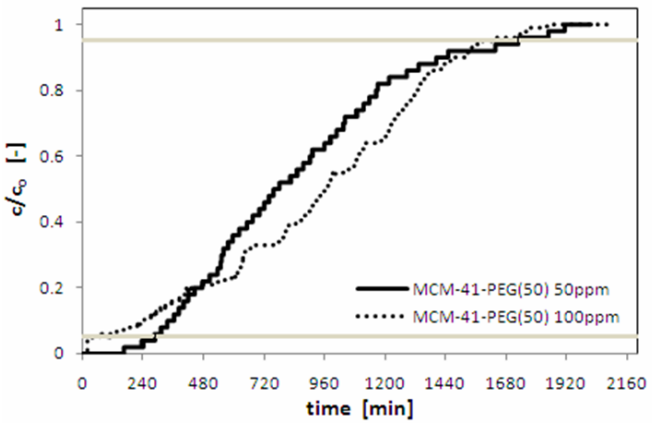

Figure 14: Breakthrough curves of NO_2/air for a sieve MCM-41-PEG(50) at concentrations of 50 ppm and 100 ppm

for the same material at 80°C the capacity was about 13 times smaller.

2.3.4. *NO_2 concentration influence on the sorption capacity of MCM-41 sieve*

In order to determine the NO_2 concentration influence on the sorption capacity, studies were carried out using NO_2 gas at concentrations of 100 ppm/air and 50 ppm/air at 25°C. Figure 14 shows the breakthrough curves for sieve MCM-41-PEG(50) for concentrations of 50 and 100 ppm.

The sorption capacity of sorbent at a concentration of 50 ppm was 0.27 mg NO_2/g of sorbent, while for the concentration of 100 ppm it was 0.31 mg NO_2/g of sorbent. Table 6 presents the data of sorption capacity for different concentrations of NO_2 gas.

As can be seen from Table 6, the sorption capacity for sieves through which the gas at concentration of 50 ppm was passed is about 5 times larger than the capacity of the sieve through which gas at a concentration of 100 ppm flowed.

Table 6: Sorption capacity for sieve MCM-41-PEG(50)

No.	Type of sorbent	The concentration of NO_2, ppm	Sorption capacity of NO_2, mg/g sorbent
1.	MCM-41-PEG(50)	50	6.65
2.	MCM-41-PEG(50)	100	1.35

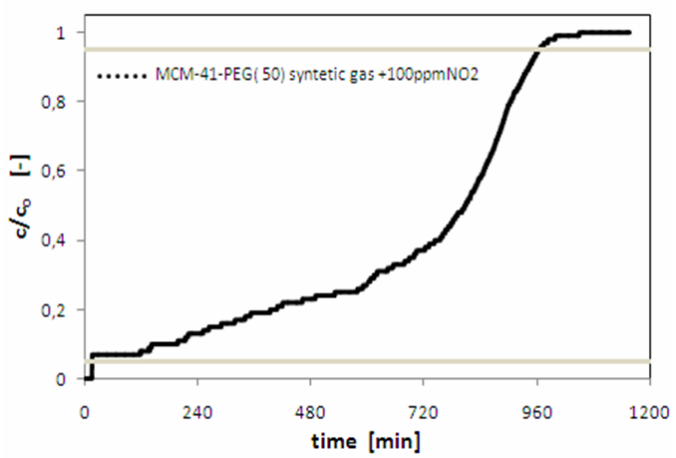

Figure 15: Breakthrough curves of NO_2/air and NO_2 + 15%, 6% O_2, 79% N_2 for a sieve MCM-41PEG(50)

2.3.5. *Influence of flue gas presence on the sorption capacity of sieve MCM-41*

The aim of this research was the application of sieves from fly ash in the process of flue gas cleaning before carbon-capture process. Due to this fact, the sorption capacity in the presence of exhaust gas components, i.e. 15% CO_2, 6% O_2, 79% N_2 was determined. Gases with the same flow stream of 0.5 l/min after mixing in the mixer were placed into the oven. The study was conducted at 25°C at a concentration of 100 ppm NO_2.

Figure 15 shows the breakthrough curves for the sieve MCM-41-PEG(50) in the flow of NO_2 and in the presence of a mixture containing carbon dioxide. The sorption capacity for sieve MCM-41 for gas NO_2 (100ppm)/air was 0.5 mg NO_2/g of sorbent, while for NO_2 in the presence of carbon dioxide it was 1.11 mg/g sorbent.

For comparison, the results of sorption capacity

Table 7: Sorption capacity sieve MCM-41 and MCM-41-PEG (50)

No.	Type of sorbent	Gas	Sorption capacity of NO_2, mg/g sorbent
1.	MCM-41	100 ppm NO_2	0.5
2.	MCM-41	100 ppm NO_2 + 15%CO_2, 6%O_2, 79%N_2	1.11
3.	MCM-41	15%CO_2, 6%O_2, 79%N_2	33.83*
4.	MCM-41-PEG(50)	50 ppm NO_2	6.65
5.	MCM-41-PEG(50)	100 ppm NO_2	1.35
6.	MCM-41-PEG(50)	100 ppm NO_2 + 15%CO_2, 6%O_2, 79%N_2	0.68
7.	MCM-41-PEG(50)	15%CO_2, 6%O_2, 79%N_2	19.51*

*CO_2 sorption capacity

for the sieve MCM-41 and MCM-41-PEG(50) were collected and presented in Table 7.

The sorption capacity of MCM-41-PEG(50) in the presence of CO_2 was 0.68 mg NO_2/g of sorbent, however for a sieve placed in a flow of NO_2 (without CO_2) at a concentration of 50 ppm NO_2 it was 6.65 mg NO_2/g of sorbent, and for a concentration of 100 ppm, 35 mg NO_2/g sorbent.

2.4. Discussion of results

The study shows that several parameters affect the sorption capacity of mesoporous materials. One is temperature. As the temperature increases, the sorption capacity of sieves for NO_2 decreases. The highest sorption capacity was observed for sieve MCM-41-PEG(50) at 25°C while at 80°C this value fell to 0.1 mg NO_2/g of sorbent.

Another parameter is the NO_2 concentration. When comparing the sorption capacity for different NO_2 concentrations, it was observed to be higher for the sieve through which gas flowed at a concentration of 50 ppm. The presented data shows that impregnating mesoporous sieves with a polyethylene glycol solution increased the sorption capacity of the sieves. The highest sorption capacity was obtained for impregnated sieves that were obtained from pure reagents and commercial sieves. However, satisfactory results were also obtained for the sieves made from fly ash.

3. Conclusion

Based on studies of both the synthesis of mesoporous materials from fly ash and the study of the adsorption process of nitrogen dioxide on the received materials, it can be seen that fly ashes from burning coal, lignite, and biomass co-firing in pulverized and fluidized bed as well, due to their significant silicon and aluminum content, are suitable materials for the synthesis of mesoporous sieves. Synthesis of mesoporous sieves from fly ash enables management of both ashes stored in landfill as well as those from current production. Modification of the ashes into the sieve allows one to obtain valuable mesoporous sorbents from the combustion of waste by-products, such as ashes, for re-use in the energy sector. Modification of materials obtained by impregnation with a polyethylene glycol solution allows one to obtain materials with enhanced properties, such as sorption capacity, relative to NO_2. The sorption capacity of impregnated sieves for NO_2 sorption was higher than for base sieves (without impregnation). The study performed at different temperatures showed that the sorption capacity of the sieve MCM-41-PEG(50) falls as temperature rises. The presence of gas with a composition of 15% CO_2, 6% O_2, 79% N_2 has only a very marginal effect on capacity.

Acknowledgments

The research was financed from the resources of Project No. N N523 482934 "Studies of adsorption

of nitrogen oxides on mesoporous materials based on fly ash".

References

[1] I. Majchrzak-Kucęba, W. Nowak, P. Sil-Ibek, B. Kucharska, Mezoporowate sita molekularne z popiołów lotnych, in: Fluidalne Spalanie Paliw w Energetyce, Materiały Konferencyjne, 2005, pp. 171–179.

[2] I. Majchrzak-Kucęba, W. Nowak, Modyfikacja popiołów lotnych w mezoporowate materiały, in: VII Ogólnopolska Konferencja Naukowo-Techniczna, Materiały Konferencyjne, 2005, pp. 309–318.

[3] H.-L. Chang, C.-M. Chun, I. A. Aksay, W.-H. Shih, Conversion of fly ash into mesoporous aluminosilicate, Ind. Eng. Chem. Res. 38 (3) (1999) 973–977. doi:10.1021/ie980275b.

[4] K. You, J. Ahn, W. Ahn, Synthesis of hexagonal and cubic mesoporous silica using power plant bottom ash, Microporous and Mesoporous Materials 111 (1–3) (2008) 455–462.

[5] I. Majchrzak-Kucęba, A. Ściubidło, W. Nowak, Studies on the properties of mesoporous materials derived from polish fly ashes, in: Proceedings of 26^{th} Annual International Pittsburgh Coal Conference, Pittsburgh, 2009.

[6] A. Ściubidło, I. Majchrzak-Kucęba, W. Nowak, Zagospodarowanie popiołów lotnych z polskich elektrowni i elektrociepłowni poprzez modyfikację popiołów w materiały mezoporowate, in: EuroCoalAsh 2008, 2008.

[7] I. Majchrzak-Kucęba, W. Nowak, Synthesis and characterization of mesoporous materials from cfb-fly ash, in: Proceedings of 9^{th} International Conference on Circulating Fluidized Beds in conjunction with the 4^{th} International VGB Workshop Operating Experience with Fluidized Bed Firing Systems, Hamburg, 2008, pp. 875–880.

[8] I. Majchrzak-Kucęba, W. Nowak, Modyfikacja popiołów lotnych w sorbenty i nanomateriały – doświadczenia laboratoryjne, in: XVI Międzynarodowa Konferencja "Popioły z energetyki", Materiały Konferencyjne, 2009.

[9] I. Majchrzak-Kucęba, W. Nowak, Properties of zeolites syntesized from fly ashes and their potential application to co_2 removal from flue gas, in: Twenty-First Annual International Pittsburgh Coal Conference-Coal-Energy and the Environment, 2004.

[10] I. Majchrzak-Kucęba, W. Nowak, A. Ściubidło, Sorbenty na bazie popiołów lotnych do wychwytywania co_2 po procesie spalania, in: EuroCoalAsh 2008, 2008.

[11] I. Majchrzak-Kucęba, W. N. D. Bukalak, Synteza materiału mezoporowatego mcm-41 z popiołów lotnych i jego zastosowanie do adsorpcji co_2, in: III Ogólnopolski Kongres Inżynierii Środowiska, Materiały Konferencyjne, Lublin, 2009.

[12] I. Majchrzak-Kucęba, W. Nowak, Development of fly ash-based sorbent to capture co_2 from flue gas, in: 20^th International Conference on Fluidized Bed Combustion, 2009.

[13] X. Xu, C. Song, R. Wincek, J. Andresen, B. Miller, A. Scaroni, Separation of co_2 from power plant flue gas using a novel co_2 "molecular basket" adsorbent, Prepr. Am. Chem. Soc. Div. Fuel Chem. 48 (2003) 162–163.

[14] X. Xu, C. Song, B. G. Miller, A. W. Scaroni, Adsorption separation of carbon dioxide from flue gas of natural gas-fired boiler by a novel nanoporous "molecular basket" adsorbent, Fuel Processing Technology 86 (2005) 1457–1472.

[15] X. Ma, X. Wang, C. Song, "molecular-basket" sorbents for co_2 capture from flue gas, in: Pittsburgh Coal Conference, 2009.

[16] I. Majchrzak-Kucęba, W. Nowak, A. Matysiak, Mezoporowate materiały z popiołów lotnych do separacji dwutlenku węgla ze spalin, in: XIV Międzynarodowa Konferencja Popioły z Energetyki, Materiały Konferencyjne, Międzyzdroje, 2007.

[17] N. Hiyoshi, K. Yogo, T. Yashima, Adsorption characteristics of carbon dioxide on organically functionalized sba-15, Microporous and Mesoporous Materials 84 (2005) 357–365.

[18] C. Govindasamy, W. Son, W. Ahn, Synthesis of mesoporous materials sba-15 and cmk-3 from fly ash and their application for co_2 adsorption, Journal of Porous Materials 16 (5).

[19] A. Ściubidło, W. Nowak, Synteza mezoporowatego sita mcm-41 z popiołów lotnych do usuwania tlenków azotu, in: XVI Międzynarodowa Konferencja Popioły z energetyki, Materiały Konferencyjne, Zakopane, 2009.

[20] X. Wang, X. Ma, S. Zhao, B. Wang, C. Song, Nanoporous molecular basket sorbent for no_2 and so_2 capture based on a polyethylene glycol-loaded mesoporous molecular sieve, Energy environ.Sci. 2 (2009) 878–882.

[21] W. Nowak, I. Majchrzak-Kucęba, Sorbenty z popiołów lotnych dla energetyki, in: XVI Międzynarodowa Konferencja Popioły z energetyki, Materiały Konferencyjne, Zakopane, 2009.

[22] I. Nowak, M. Ziółek, Uporządkowane materiały mezoporowate, Wydawnictwo Uniwersytetu Wrocławskiego, Wrocław, 2001.